ISSN 1052-6188, Journal of Machinery Manufacture and Reliability, 2018, Vol. 47, No. 2, pp. 196–204. © Allerton Press, Inc., 2018.
Original Russian Text © I.N. Andronov, M.Yu. Demina, L.S. Polugrudova, 2018, published in Problemy Mashinostroeniya i Nadezhnosti Mashin, 2018, No. 2, pp. 75–83.

EXPERIMENTAL MECHANICS, DIAGNOSTICS, AND TESTING

Method for Designing Springs Using Materials with Shape Memory as the Actuators of Power Units

I. N. Andronov[a], M. Yu. Demina[b,*], and L. S. Polugrudova[b]

[a] *Ukhta State Technical University, Ukhta, Russia*

[b] *Syktyvkar Forest Institute, St. Petersburg State Forest Technical University, Syktyvkar, Russia*

**e-mail: mdemina59@mail.ru*

Received February 17, 2017; in final form, November 20, 2017

Abstract—The physical and mechanical behavior of titanium nickelide coil springs of different stiffness is experimentally investigated during thermal cycling through martensitic transformation ranges under a constant tensile force. The springs exhibit a reversible length change by reciprocating movements. In terms of classical mechanics, a method for the design calculation of springs with shape memory as actuators is proposed for a given stiffness range.

DOI: 10.3103/S1052618818020024

A coil spring is a traditional and well-studied form of the operating element of devices. Springs made of structural materials are considered as elastic bodies for the accumulation of energy under the action of a load and capable of converting the accumulated energy in a reversible form after the termination of the load. The spring, as an integral part, is used in a variety of mechanisms to excite motion because of reverse motion, measurement of loads, and damping of shocks and impacts. The existing theoretical models of structural springs are well developed and based on the plane section method. They also assume that in the case of spring deformation the displacements are small, the turn inclination angle does not exceed 12°, and the spring diameter barely changes [1–4]. Under such assumptions, only the torque is important among the cross-sectional forces. The longitudinal and transverse forces, as well as the bending moment, are neglected. According to the developed methods for calculating the structural spring elements, the tables *Parameters of springs* are compiled, in which the optimal geometric parameters of the springs of certain classes are given in the range of the planned loads. Therefore, the design calculation algorithm is the selection of the spring according to the given initial data: the load, working stroke, and preliminary external diameter. Further, according to the determined class and discharge of the spring, its stiffness is found and the remaining dimensions of the attachment are calculated.

The functions fulfilled by alloys through shape memory can be extended due to the unique properties of the materials themselves. The possibilities alloys with shape memory are due to the shape memory effect (SME) observed in them, which is the restoration of a predetermined deformation upon subsequent heating. The restored deformation can reach up to ~10%. If we limit the restoration of the shape of the deformed material, then reactive stresses of 600–700 MPa arise. The phase yield strength of alloys with shape memory in the martensitic state corresponds to approximately 80–100 MPa [5]. Due to these unique properties, alloys with shape memory are used in actuators, automatic sensors, switches, controllers, etc. The prospects for the use of coil springs made from alloys with shape memory continue to attract interest in the development of methods and approaches to calculate such structures [6–10].

The behavior of springs under the action of tensile forces is as follows. Under the action of the torque created by the tensile force, twisting and bending moments acting in the vertical plane occur in the cross sections of the spring's flexible rod [1–4]. The specified internal force factors ensure the action of shear and normal stresses in the cross sections of the spring, in the direction of which the plasticity of the direct transformation occurs [1]; i.e., martensite crystals grow toward internal microforces. Subsequent heating through the inverse martensitic transformation range leads to the inverse process, i.e., the SME in the opposite direction. At the same time, the deformation process upon heating occurs with strict adherence to the crystal's geometric principle "exactly backward," theoretically grounded by Professor V.A. Likhachev at Leningrad State University, and his students in [11]. It follows from [11] that in terms of energy the reverse transformation is more advantageous, when the distortions during heating are equal

to the distortions of the direct transformations. In this case, the boundaries of the twins and the orientation variants of martensite are not inherited by austenite. The crystal's noted geometric principle "exactly backward" provides a complete deformation relief in the case of a reverse transformation. Obviously, this is true when the values of the effective stresses are small and do not exceed the value of the phase yield strength.

Coil springs made of alloys with shape memory feature a change in the number of active turns, the turn diameter, the turn inclination angle, and the shear modulus of the material during a deformation by a constant axial load under changing temperatures. The existing calculation methods usually take into account a change in one or two factors, and do not make it possible to carry out a design calculation of a spring made from an alloy with shape memory.

The purpose of this investigation is to develop a method for designing springs with a shape memory used as actuators of power units. The following problems are solved in the paper: the experimental study of the deformation-force behavior of springs with shape memory of different stiffnesses and the development of an algorithm for the design calculation of springs with shape memory as actuators of power units.

EXPERIMENTAL

In the experiments we used coil spiral springs made of an equiatomic TiNi wire with a diameter of $d =$ 2 mm. For this material, the temperatures of the martensitic transformations are $M_s = 323$ K, $M_f = 303$ K, $A_s = 328$ K, and $A_f = 348$ K. The production method of springs and the experimental procedure are described in detail in [12, 13]. Two springs with different initial operating parameters were tested: with the outer diameter D_0 of the turn in the spring and the spring index $C = (D_0 - d)/d$; and with the initial number of turns n_0 and stiffness c. Spring 1 parameters: $D_0 = 27$ mm, $C = 12.5$, $n_0 = 22$, $c = 174.55$ N/m. Spring 2 parameters: $D_0 = 20$ mm, $C = 9$, $n_0 = 23$, $c = 447.31$ N/m.

The initial spring stiffness was determined by the following formula:

$$c = \frac{Gd^4}{8(D_0 - d)^3 n} = \frac{Gd}{8C^3 n},$$

where G is the shear modulus of titanium nickelide in the martensitic state. According to [5], it is $G = 30$ GPa.

The experiments were carried out as follows. The spring was heated to a temperature $T_{\max} = 363$ K, and then in the austenite state, it was loaded by tensile force $P_i = 1.0$, 1.5, 2.0, 2.5, 3.0, 3.5, 4.0, and 4.5 N. Then, the spring was cooled through the full martensitic transformation range to a temperature of $T_{\min} =$ 297 K and subsequently heated. In the course of the thermal cycle, the temperature T was measured by the chromel-copel thermocouple fixed to the spring, as well as the spring elongation $\delta(T, P_i)$ corresponding to it and the load. The experiments carried out by the described scheme were repeated thrice for each spring. The average value of the elongation δ was taken as the main experimental parameter. The error was measured in accordance with the rules for processing direct measurements using Student's test. The bias was $\Delta\delta_{\text{bias}} = 1$ mm, the random error was calculated as $\Delta\delta_{\text{rand}} = t_{\alpha,N}\sqrt{\sum_N (\delta_i - \overline{\delta})^2/(N(N-1))}$, where Student's coefficient was taken as $t_{\alpha,N} = 2.92$ for the confidence probability $p = 0.9$ and the number of experiments $N = 3$. The maximum value of the random error under such parameters was $\Delta\delta_{\text{rand}} = 2.3$ mm, and the total error did not exceed 17%.

According to the experimental procedure considered in [12, 13], the spring was subjected to isothermal deformation in austenite at the initial loading stage, then it was stretched due to the plasticity of the direct transformation during cooling under load. At the first stage of loading by the tensile force in the austenitic state at $T_{\max} = 363$ K, the spring's compression δ^A was determined by the axial force and the spring's parameters (Table 1). For example, spring 1 under a load of 4 N was stretched in austenite by 64% and the compression of spring 2 was 29%. The experimental data were processed by the methods of correlation and regression analysis. The coefficient of linear correlation of the dependence $P = f(\delta^A/l_0)$ was 0.98–0.99, which indicated the elastic deformation of the springs in austenite. This conclusion is confirmed by [14], in which it was experimentally shown that in the austenitic phase the linear region of the force–relative deformation dependence of the spring can reach 200%.

Table 1. Dependence of elongation of springs under load in austenite δ^A and maximum elongation during cooling under load δ from applied tensile force

P, N	Spring no. 1		Spring no. 2	
	δ^A, %	δ, %	δ^A, %	δ, %
1.0	6.82	340.91	2.78	71.74
1.5	15.91	615.91	6.94	100.00
2.0	22.73	875.00	13.89	217.39
2.5	34.09	1118.18	16.67	278.26
3.0	47.73	1411.36	20.83	395.65
3.5	56.82	1625.00	26.39	469.57
4.0	63.64	1813.64	29.17	573.91
4.5	77.27	1959.09	34.72	669.57

After the loading stage, the springs were cooled under the applied axial tensile force. For spring 1, which is the least stiff spring, the ratio of the maximum elongation accumulated during the transformation plasticity stage to the initial length of the undeformed spring under a load of 4.5 N is more than 1900%. For spring 2, it is 670%. Table 1 shows the values of the greatest relative elongation of the springs at the cooling stage under the axial tension force. It can be seen that the change in the length of the TiNi spring during thermal cycling in the loaded state through the austenitic–martensitic transformation range is significant even under small tensile forces. Despite such a significant elongation, the deformation due to the transformation plasticity was almost completely restored on subsequent heating under load due to the SME.

Figure 1 shows the change in the average elongation δ for spring 1 during thermal cycling under the action of the axial load without taking into account the spring's compression during the isothermal loading stage. The relative elongation of the spring during the cooling stage under the load for an axial force

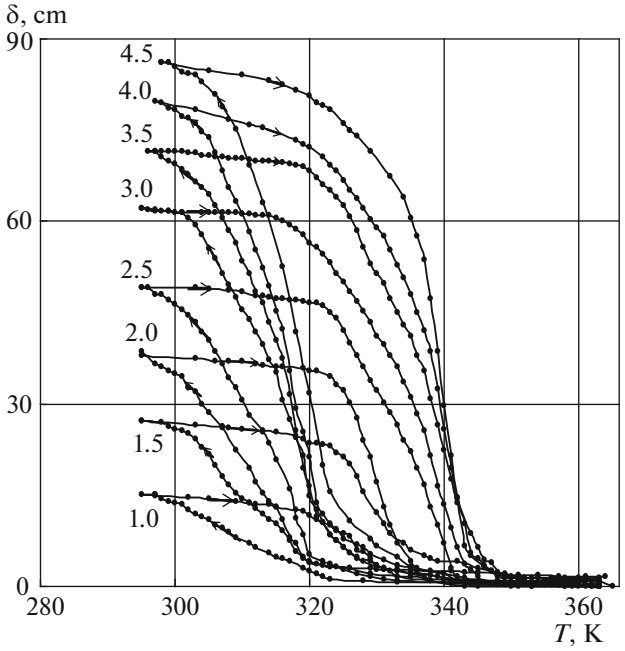

Fig. 1. Spring elongation δ during thermal cycling under load (tensile force values are given in N and indicated by figures near curves).

of 1 N was 341% (the displacement of the free end of the spring of $\delta_{1,0} = 150$ mm and the initial spring length was 4.4 cm), and for a force of 4.5 N, it reached 1960% ($\delta_{4,5} = 862$ mm).

COMPUTATIONAL AND ANALYTICAL

Algorithm for Determining Stresses and Deformations

The values of the stresses and deformations in the inner and outer fibers of the spring were determined by the method described in [12, 13]. In the method presented in [12], the shear deformation and shear stress due to the twisting of the wire, as well as the axial deformation and normal stress caused by the bending, are taken into account.

Let us give a sequence of calculations of the stresses and deformations arising in the spring material during the thermal cycle under load. The initial parameters for the calculation are the wire diameter d, the initial diameter of the spring turn $D_0 = D_{\max}$, the initial spring stiffness $C = (D_0 - d)d$, and the initial number of active turns n_0. We experimentally determine the current elongation $\delta(T, P_i)$, the maximum elongation $\delta_i^{\max}(P_i)$, and the minimum diameter $D_i^{\max}(P_i)$ under the specific tensile force $P_i = \text{const}$. The discrete auxiliary function is calculated based on the results of the experiment:

$$f(P_i) = \frac{D_{\max} - D_i^{\min}(P_i)}{\delta_i^{\max}(P_i)},$$

it is used to determine the current turn diameter during the cooling and heating stages, respectively:

$$D_{\text{cool}}(T, P_i) = D_{\max} - f(P_i)\delta_{\text{cool}}(T, P_i), \quad D_{\text{heat}}(T, P_i) = D_{\max} - f(P_i)\delta_{\text{heat}}(T, P_i).$$

Then, for the given temperature and tensile force, we determine the number of active turns

$$n(T, P) = \frac{-d\delta/\pi^2 + \sqrt{d^2\delta^2/\pi^4 - ((D-d)^2 + d^2/\pi^2)(\delta^2/\pi^2 - ((D_0 - d)^2 + d^2/\pi^2)n_0^2)}}{(D-d)^2 + d^2/\pi^2},$$

shear deformation

$$\gamma(T, P_i) = \frac{d}{D}\left(\arctan\frac{d + \delta/n}{\pi(D-d)} - \arctan\frac{d}{\pi(D_0 - d)}\right),$$

axial deformation

$$\varepsilon(T, P_i) = \frac{(D-d)d}{(D-d)^2 + (d + \delta/n)^2/\pi^2} - \frac{(D_0 - d)d}{(D_0 - d)^2 + (d/\pi)^2},$$

normal stress

$$\sigma_{\text{outer}}(T, P_i) = \frac{16P(D-d)[(d + \delta/n)/(\pi(D-d))]}{\pi d^3\sqrt{1 + (d + \delta/n)^2/(\pi(D-d))^2}},$$

and the shear stress in the outer fiber

$$\tau_{\text{outer}}(T, P_i) = k_s\frac{8P(D-d)}{\pi d^3\sqrt{1 + (d + \delta/n)^2/(\pi(D-d))^2}},$$

where the correction factor for the shear stress is $k_s = (D-d)/D$.

Calculation of Stresses and Deformations

According to [12, 13], the shear deformation related to the surface fibers of the spring is determined by the following formula:

$$\gamma = \frac{d}{2\pi(D-d)}\left(\arctan\frac{d + \delta/n}{\pi(D-d)} - \arctan\frac{d}{\pi(D_0 - d)}\right), \quad (1)$$

where n is the current number of turns.

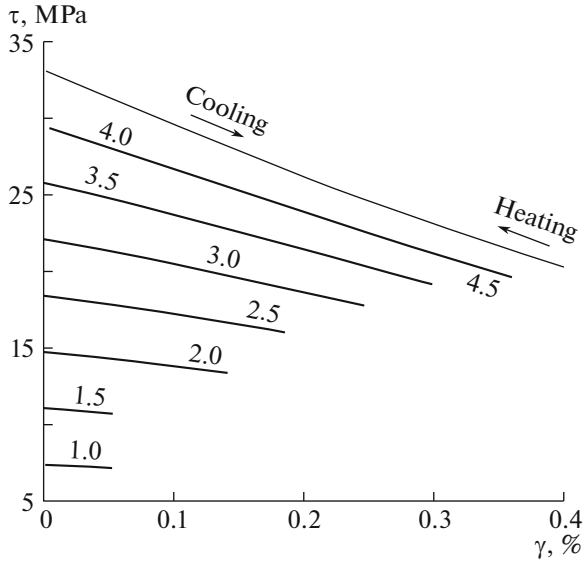

Fig. 2. Isolines of thermal cycle in coordinates $\gamma - \tau$ for spring with stiffness $c = 174.55$ N/m (tensile force values are given in N and indicated by figures).

A comparison of [1] and [2] makes it possible to write the shear stress in the outer fiber (the farthest from the center line) as follows:

$$\tau_{\text{outer}}^{\max} = k_s \frac{8P(D-d)}{\pi d^3 \sqrt{1 + d^2/(\pi(D-d))^2}} = \frac{D+d}{d} \frac{8P(D-d)}{\pi d^3 \sqrt{1 + d^2/(\pi(D-d))^2}}.$$

For the inner fiber, the coefficient k_s can be expressed in terms of the spring index in the following form:

$$k_s = \frac{D_0 - d}{d} = \frac{Cd}{(C+1)d} = \frac{C}{C+1}.$$

Then the stresses in the inner fiber (closest to the center line) will be represented by the following dependence:

$$\tau_{\text{inner}}^{\max} = \frac{C+1}{C-1}\tau_{\text{outer}}^{\max} = \frac{C+1}{C-1}\frac{C}{C+1}\frac{8P(D_0-d)}{\pi d^3 \sqrt{1 + (1/\pi C)^2}} = \frac{C}{C-1}\frac{8P(D_0-d)}{\pi d^3 \sqrt{1 + (1/\pi C)^2}}. \quad (2)$$

This stress is limited to the maximum value of τ_1 obtained from the experimental-calculation results:

$$\tau_{\text{inner}}^{\max} = \frac{C+1}{C-1}\tau_{\text{outer}}^{\max} = \frac{C}{C-1}\frac{8P(D_0-d)}{\pi d^3 \sqrt{1 + (1/\pi C)^2}} \le \tau_1. \quad (3)$$

According to formulas (1) and (3), the hysteresis curves corresponding to the constant tensile force P_i were recalculated in the isoline of the thermal cycle in th coordinates $\gamma - \tau$ represented for the spring stiffnesses of 174.55 N/m (Fig. 2) and 447.31 N/m (Fig. 3). It is clearly seen from the shape of the curves in Figs. 2 and 3 that during the thermal cycle, under a constant tensile force, the shear stresses decrease according to a law that is close to linear as the shear deformation increases. It is characteristic that the

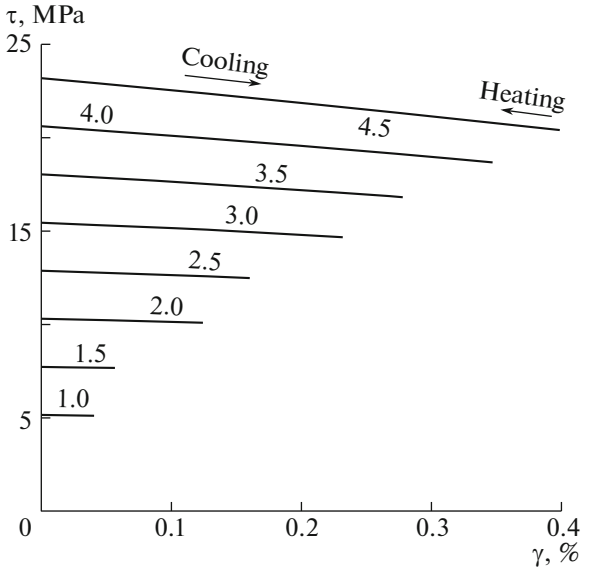

Fig. 3. Isolines of thermal cycle in coordinates $\gamma - \tau$ for spring with stiffness $c = 447.31$ N/m (tensile force values are given in N and indicated by figures).

intensity of the stress change along the deformation $\left|\frac{d\tau}{d\gamma}\right|$ turns out to be much higher for a less stiff spring (Fig. 2) than the corresponding values for a stiffer spring (Fig. 3).

Spring Design

The task was to develop an algorithm for designing a spring using material with the SME for the given initial data: P is the value of the constant tensile force acting during thermal cycling, δ is the maximum elongation of the spring during thermal cycling through the martensitic transformation ranges under load P, C is the spring index, and G is the shear modulus of titanium nickelide in the martensitic state. A fixed value of the shear modulus corresponding to the martensitic state of the TN-1 alloy was used in the calculations [15] $G = 30$ GPa, initial values of other parameters: $P = 4$ N, $\delta = 25$ mm, and $C = 10$.

The isolines $\gamma - \tau$ shown in Figs. 2 and 3 make it possible to solve the problem of the design calculation of a spring made of the specified material for design forces within the range $1.0 \text{ N} \le P \le 4.5$ N. It can be seen that the shear stress and the shear deformation change during the thermal cycling under a constant axial force. The two most important isolines are taken from the total number of obtained curves that correspond to the force $P = 4$ N for springs with stiffness $c_1 = 174.55$ N/m and $c_2 = 447.31$ N/m (Fig. 4). It is obvious that for the subsequent design calculation, the maximum shear stress found by formula (2) will be the most important one. It will be $\tau_1^{\max} = 30$ MPa and $\tau_2^{\max} = 20$ MPa, respectively. A careful analysis of the type of experimental isolines in Figs. 2 and 3 makes it possible to assume that the maximum shear stresses are related to the spring stiffness by the following dependence:

$$\tau^{\max} = \frac{A}{c^{\alpha}}, \tag{4}$$

where A and α are some constants of the material and $\tau^{\max}$ is the maximum possible stress applied during the thermal cycling of the spring with stiffness c.

We find the constant α from the following equation:

$$\alpha = \frac{\ln(\tau_1^{\max}/\tau_2^{\max})}{\ln(c_2/c_1)},$$

then using (4) we determine A.

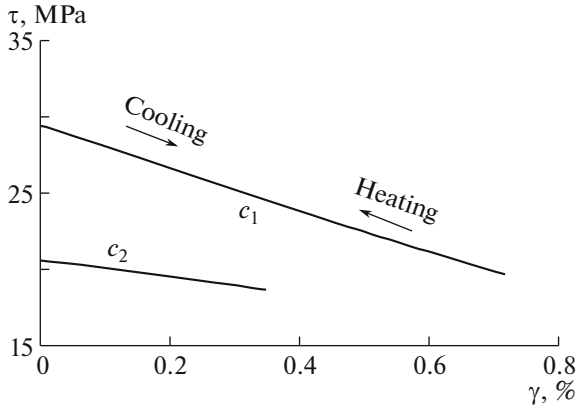

Fig. 4. Isolines of thermal cycle in coordinates $\gamma - \tau$ for springs with different stiffness for tensile force $P = 4$ N: $c_1 =$ 174.55 N/m and $c_2 = 447.31$ N/m.

Similarly, let us introduce the relationship between the angular deformation and the spring stiffness

$$\gamma^{\max} = B/c^{\beta}, \tag{5}$$

where B and β are some constants of the material and $\gamma^{\max}$ is the maximum possible deformation accumulated during the thermal cycling of the spring with stiffness c.

We find the constant β from the following equation:

$$\beta = \ln(\gamma_1^{\max}/\gamma_2^{\max})/\ln(c_2/c_1)$$

then, using (5) we determine B.

The results of the calculation of the constants are given in Table 2. The values of $\tau^{\max}$ and $\gamma^{\max}$ for the tensile force $P = 4$ N are determined for springs with the known stiffness c by the graphs in Fig. 4.

Let us write down the shear stress constraint condition $\tau^{\max}$ (an analog of the strength condition)

$$\tau_{\text{inner}}^{\max} = \frac{C}{C-1}\frac{8P(D_0 - d)}{\pi d^3\sqrt{1 + (1/\pi C)^2}} = \frac{8PC}{\pi d^2\sqrt{1 + (1/\pi C)^2}} \le \tau^{\max}.$$

Then the wire thickness can be determined from the condition

$$d \ge C\sqrt{\frac{8P}{\tau^{\max}(\pi^2 + 1/C)^2}}.$$

The number of given turns is determined from the condition of the angular deformation constraint

$$\gamma = \frac{d}{2\pi(D-d)}\left(\arctan\frac{d + \delta/n}{\pi(D-d)} - \arctan\frac{d}{\pi(D_0 - d)}\right) \le \gamma_{\max},$$

Table 2

Quantity	Spring 1	Spring 2
c, N/m	174.55	447.31
$\tau^{\max}$, MPa	30.00	20.00
$\gamma^{\max}$, %	0.80	0.40
α	0.43	
A	277.38	
β	0.74	
B	35.84	

Table 3

Quantity	Approximation					
	1	2	3	4	5	6
c_i, N/m	310.93	400.11	423.04	430.14	432.40	433.13
τ^{max}, MPa	23.39	20.98	20.49	20.34	20.29	20.28
d, mm	1.99	2.10	2.13	2.13	2.14	2.14
γ^{max}, %	0.52	0.43	0.42	0.41	0.41	0.41
n	11.46	13.27	13.70	13.83	13.87	13.88
c_f, N/m	489.29	445.98	437.23	434.67	433.87	433.61
$(c_f - c_i)/c_i$, %	57.36	11.47	3.35	1.05	0.34	0.11

where γ_{max} is the greatest deformation during thermal cycling, which for a spring of a certain stiffness, is found from the graphs in Fig. 4.

The formula for calculating the number of turns for a known maximum elongation δ during thermal cycling (6) follows from the condition given above:

$$n \geq \frac{\delta}{d}\left(\frac{\pi C \tan(2\pi C\gamma_{max}) + 1}{1 - (1/(\pi C))\tan(2\pi C\gamma_{max})} - 1\right)^{-1}.$$

The calculation is carried out by the method of successive approximations. At each stage we successively calculate c, τ, d, γ, and n and check the convergence with respect to the spring stiffness c.

Table 3 shows the results of calculating the parameters of the designed spring at each step with a check for the convergence of the solution with respect to the spring stiffness.

Based on the results of the calculations, the final design parameters of the spring are as follows: d = 2.14 mm, D = 21.4 mm, and n = 13.88.

Thus, the proposed method for the design calculation of titanium nickelide coil springs is likely to be applied in engineering when designing actuators of materials with SME.

REFERENCES

1. *Raschety na prochnost' v mashinostroenii. T. 1. Teoreticheskie osnovy i eksperimental'nye metody. Raschety sterzhnevykh elementov konstruktsii pri staticheskoi nagruzke* (Strength Calculations in Mechanical Engineering, Vol. 1: Theoretical Principles and Experimental Methods. Calculations of Structural Bars under Static Load), Ponomarev, S.D., Ed., Moscow: Mashgiz, 1956.
2. Ponomarev, S.D. and Andreeva, L.E., *Raschet uprugikh elementov mashin i priborov* (Calculation of Elastic Elements of Machines and Devices), Moscow: Mashinostroenie, 1980.
3. *Mashinostroenie: entsiklopediya, Kn. 1. Dinamika i prochnost' mashin. Teoriya mashin i mekhanizmov* (Machinery, Encyclopedy, Vol. 1: Dynamics and Strength of Machines. The Theory of Machines and Mechanisms), Frolov, K.V. et al., Eds., Moscow: Mashinostroenie, 1994.
4. Feodos'ev, V.I., *Soprotivlenie materialov* (Material Resistance), Moscow: Mosk. Gos. Tekh. Univ. im. N.E. Baumana, 1999.
5. Likhachev, V.A., Kuz'min, S.L., and Kamentseva, Z.P., *Effekt pamyati formy* (Shape Memory Effect), Leningrad: Leningr. Gos. Univ., 1987.
6. Movchan, A.A., Mozafari, A., and Kazarina, S.A., Analysis of the activator work with shape memory alloy spring, *Izv. Vyssh. Uchebn. Zaved., Aviats. Tekh.,* 1999, no. 4, pp. 20–23.
7. Mandzhavidze, A.G., Barnov, V.A., Sobolevskaya, S.V., and Margvelashvili, O.V., Shape memory materials as a working substance for martensitic rotary engines, *Tech. Phys.,* 2006, vol. 51, no. 5, pp. 663–665.
8. Abdrakhmanov, S.A., Dotalieva, Zh.Zh., Kozhoshov, T.T., and Zhanaliev, N.R., Analytical investigation of characteristics of cylindrical springs with shape memory, *Mekh. Kompoz. Mater. Konstrukts.,* 2010, vol. 16, no. 1, pp. 165–171.

9. Gavryushin, S.S. and Ganysh, S.M., Numerical simulation of deformation processes of the element in the form of a helical coil spring made of a shape memory material, *Izv. Vyssh. Uchebn. Zaved., Mashinostroen.,* 2012, no. 8, pp. 15–20.
10. Auricchio, F., Scalet, G., and Urbano, M., A numerical/experimental study of nitinol actuator springs, *J. Mater. Eng. Perform.,* 2014, vol. 23, no. 7, pp. 2420–2428.
11. Brainin, G.E., Volkov, A.E., and Likhachev, V.A., The inheritance of twin boundaries as a shape memory mechanism, *Fiz. Met. Metalloved.,* 1982, vol. 55, no. 6, pp. 1045–1050.
12. Andronov, I.N., Demina, M.Yu., and Polugrudova, L.S., Calculation-experimental analysis of the thermocyclic deformation of titanium nickelide coil springs, *Russ. Metall. (Metally),* 2016, no. 4, pp. 300–306.
13. Demina, M.Yu., Andronov, I.N., and Polugrudova, L.S., Influence of design parameters of NiTi tension spring on strain and stress arising at intervals during thermal cycling of martensitic transformations, *Deform. Razrush. Mater.,* 2015, no. 6, pp. 20–24.
14. Manjavidze, A.G., Barnov, V.A., Jorjishvili, L.I., and Sobolevskaya, S.V., Appearance of the two way shape memory effect in a nitinol spring subjected to temperature and deformation cycling, *Tech. Phys.,* 2008, vol. 53, no. 3, pp. 380–382.
15. Andronov, I.N., Bogdanov, N.P., and Tarsin, A.V., The effect of the character of temperature-cycle tests and sign of loading on the value of phase modulus of titanium nickelide, *Zavod. Lab., Diagn. Mater.,* 2009, vol. 75, no. 4, pp. 42–44.

Translated by O. Pismenov